Deuteron breakup at extreme forward angles: Failure of a pure Coulomb dissociation description

C. Samanta,* Sanjukta Mukherjee, and Rituparna Kanungo
Saha Institute of Nuclear Physics, 1/AF, Bidhan Nagar, Calcutta-700064, India

D. N. Basu
Variable Energy Cyclotron Centre, 1/AF, Bidhan Nagar, Calcutta-700064, India

(Received 19 May 1995)

We present an analysis of recent measurement of the 56 MeV deuteron breakup data on ^{12}C, ^{40}Ca, and ^{208}Pb targets taken by Okamura *et al.*. The cross section measured at $\theta_p = \theta_n = 0°$ was claimed to be a strong evidence of Coulomb breakup, especially in light nuclei. However, the single-step pure Coulomb breakup formalism fails to describe both the magnitude and the shape of the triple differential cross section even in light nuclei. At 56 MeV incident deuteron energy, the nuclear interference effect is found to be significant in all the above nuclei. The prior form distorted-wave Born-approximation calculations with unusual optical potentials in the exit channel can reproduce the highly asymmetric shapes of the triple differential cross section at the extreme forward angle, but, fail to give their exact magnitude. The possible role of multistep processes is discussed. [S0556-2813(96)01205-8]

PACS number(s): 25.70.Mn, 24.10.Eq, 24.50.+g

I. INTRODUCTION

In recent years Coulomb dissociation [1–3] of both stable and exotic nuclei [4–7] with incident energies above the Coulomb barrier has opened up a vast area of research in the so-called ''low energy'' domain of nuclear physics. The dissociation of an energetic projectile in the intense Coulomb field of a target nucleus is an inverse process to capture reaction and it can provide important insight into the nucleosynthesis in the early Universe [8, 9]. However, a persistent problem in this quest remains in the identification of the angular region where the nuclear breakup effect can be ignored in comparison to the dominant Coulomb dissociation. Due to the short range nature of the nuclear field one usually expects less and less nuclear contribution at larger impact parameters. On the other hand, the infinite range Coulomb field of the target nucleus, although it diminishes in strength with increasing impact parameter (l), can cause significant dissociation of the projectile at large l without causing large angular deflection of the fragments. The breakup cross section at very small angle is therefore expected to be dominated by the Coulomb dissociation. However, nuclear interference effects, target-fragment final state interaction (FSI) as well as recombination of the fragments with small relative energy might cause significant changes in the expected Coulomb breakup cross section.

In the early 1980's the $d \rightarrow p+n$ breakup data on several targets provided excellent testing ground for various available theories of breakup [10–12]. The post form distorted-wave Born-approximation (DWBA) theory [10], although generally successful for low relative angles of fragments, uses a zero-range approximation, completely neglects the final state interaction and treats Coulomb breakup insufficiently. The prior form DWBA theory [11] on the other hand includes final state interaction between the breakup fragments to all orders and encompasses the full finite range effects correctly. Also, the prior form DWBA theory treats nuclear and Coulomb breakup on the same footing and was found to be quite successful for the 56 MeV $d \rightarrow p+n$ breakup except at equal-angle angle pairs where a large overprediction by the theory neccesitated an arbitrary renormalization of the calculated results to fit the data [12]. Iseri *et al.* [13, 14] demonstrated the importance of multistep processes in breakup and a rigorous coupled-channel calculation with continuum-continuum coupling reasonably reproduced the magnitude of the above data. However, the Coulomb breakup was not incorporated in their work. Later on Austern suggested that the effects of multistep processes can be simulated through an unusual optical potential at the exit channel [15].

Recently, for the first time, the 56 MeV $d \rightarrow p+n$ breakup data have been obtained at $\theta^L = \theta_p = \theta_n = 0°$ for ^{12}C, ^{40}Ca, ^{90}Zr, and ^{208}Pb targets [1]. These newly obtained data show a very interesting feature. With the lightest target ^{12}C, the $\theta^L = 0°$ data exhibit the characteristic double-peaked structure of the Coulomb dissociation not observed in the earlier larger angle data. The observed structure of energy sharing spectra at $\theta^L = 0°$ is highly asymmetric and varies in shape with the target Z-value. The two-peaked feature observed with the $Z=6$ (^{12}C) target reduces to almost one peak as the Z value increases to $Z=82$ (^{208}Pb) [1]. This immediately raises the question whether this asymmetry results from pure Coulomb dissociation or from Coulomb plus other processes mentioned earlier causing piling up of the protons at the higher energy side.

To appreciate the effects of the multistep processes at $\theta^L = 0°$ one would need a coupled discretized continuum channels (CDCC) calculation in which the Coulomb effects are properly incorporated. Unfortunately, no such calculation

*Electronic address: chhanda@hp1.saha.ernet.in

is available so far. To test the extent of validity of the one-step pure Coulomb dissociation description of the $\theta^L=0°$ data we have carried out an extensive study of the 56 MeV $d\rightarrow p+n$ breakup with ^{12}C, ^{40}Ca, and ^{208}Pb targets in the framework of the prior form DWBA theory.

A brief description of the theory is given in Sec. II to discuss its inherent limitations when applied to this work. The details of the analysis and the possible implications of the results are given in Secs. III and IV, respectively.

II. FORMALISM

The Hamiltonian for the elastic breakup process

$$a(=b+x)+A\rightarrow a^*+A\rightarrow b+x+A \tag{1}$$

can be written as

$$\begin{aligned}H=&H_A+H_b+H_x+T_b+T_x+U_{bA}(\vec{r}_{bA})+V_{bA}(\vec{r}_{bA})\\&+U_{xA}(\vec{r}_{xA})+V_{xA}(\vec{r}_{xA})+U_{bx}(\vec{r}_{bx})+V_{bx}(\vec{r}_{bx}),\end{aligned} \tag{2}$$

where H_A, H_b, H_x are the internal Hamiltonians of A, b, and x. The T_b and T_x denote the kinetic energies of fragments b and x of mass m_b and m_x, respectively, U_{bA}, U_{xA} the nuclear interaction potentials of the breakup fragments with the target A, and U_{bx} is the nuclear interaction potential which binds b and x in the projectile a with a ground state wave function $\phi_a(\vec{r})$. The V's are the respective Coulomb interaction potentials.

The prior form theory of breakup [11] includes the final state interaction between the broken up fragments b and x to all orders by virtue of the explicit use of the continuum relative wave function. The $\mathscr{T}$ matrix in the prior form can be written as [15]

$$\begin{aligned}\mathscr{T}^{\text{prior}}=&\langle\chi_{a*}^{(-)}(\vec{K}_f,\vec{R})\phi_{a*}^{(-)}(\vec{k},\vec{r})|U_{bA}(r_{bA})+U_{xA}(r_{xA})\\&+V_{bA}(r_{bA})+V_{xA}(r_{xA})-U_{aA}(r_{aA})\\&-V_{aA}(r_{aA})|\Psi^{(+)}(\vec{K}_i,\vec{r},\vec{R})\rangle.\end{aligned} \tag{3}$$

Here the target nucleus is assumed to be at rest at the origin, so that the usual coordinates are $\vec{R}=\vec{r}_{aA}=(m_b\vec{r}_{bA}+m_x\vec{r}_{xA})/(m_b+m_x), \vec{r}=\vec{r}_{bx}=\vec{r}_{bA}-\vec{r}_{xA}$, $\phi_{a*}^{(-)}(\vec{k},\vec{r})$ is the $b+x$ final state wave function. The $\chi_a^{(+)}$ and $\chi_{a*}^{(-)}$ describe the motion of the center of mass of b and x with momenta K_i and K_f at the entrance and exit channels, respectively.

The full wave function $\Psi^{(+)}$ can be explained as

$$\Psi^{(+)}=\phi_a\chi_a^{(+)}+\int dk'\,\phi_{k'}^{(+)}\chi_{k'}^{(+)}. \tag{4}$$

The DWBA expression of the $\mathscr{T}$ matrix in the prior form is obtained by taking only the first term of (4) and is written as

$$\begin{aligned}\mathscr{T}_{\text{DWBA}}^{\text{prior}}=&\langle\chi_{a*}^{(-)}(\vec{K}_f,\vec{R})\phi_{a*}^{(-)}(\vec{k},\vec{r})|U_{bA}(r_{bA})+U_{xA}(r_{xA})\\&+V_{bA}(r_{bA})+V_{xA}(r_{xA})-U_{aA}(r_{aA})\\&-V_{aA}(r_{aA})|\phi_a(\vec{r})\chi_a^{(+)}(\vec{K}_i,\vec{R})\rangle.\end{aligned} \tag{5}$$

Austern pointed out in [15] that one needs to choose a proper exit channel potential to minimize the effect of replacing $\Psi^{(+)}(\vec{K}_i,\vec{r},\vec{R})$ by $\phi_a(\vec{r})\chi_a^{(+)}(\vec{K}_i,\vec{R})$ in (5) and the potential $U_{aA}+V_{aA}$, determined by the continuum-continuum coupling term of the three-body model (as is indeed appropriate for an optical interaction in a three-body continuum), is quite different from usual optical model potential.

An alternative prior form $\mathscr{T}$ matrix [16] with a different choice of product wave functions in the exit channel is

$$\begin{aligned}\mathscr{T}=&\int\chi_b^{(-)*}(\vec{r}_{bA})\chi_x^{(-)*}(\vec{r}_{xA})[U_{bA}(r_{bA})+U_{xA}(r_{xA})\\&+V_{bA}(r_{bA})+V_{xA}(r_{xA})-U_{aA}(r_{aA})-V_{aA}(r_{aA})]\\&\times\phi_a(\vec{r}_{bx})\chi_a^{(+)}(\vec{r}_{aA})d\vec{r}_{aA}d\vec{r}_{bx},\end{aligned} \tag{6}$$

where U's are the nuclear potentials and V's are the Coulomb potentials and χ_b and χ_x are the scattering wave functions governed by the potentials $U_{bA}(r_{bA})+V_{bA}(r_{bA})$ and $U_{xA}(r_{xA})+V_{xA}(r_{xA})$, respectively. The $\phi_a(r_{bx})$ is the ground state wave function of the projectile and χ_a is the incoming wave function distorted by the potential $U_{aA}(r_{aA})+V_{aA}(r_{aA})$. This form is equivalent to the so-called post form DWBA $\mathscr{T}$ matrix [15]. The above $\mathscr{T}$ matrix can be rewritten as

$$\begin{aligned}\mathscr{T}=&\langle\chi_b^{(-)}(\vec{r}_{bA})\chi_x^{(-)}(\vec{r}_{xA})|U_{bA}(\vec{r}_{bA})+V_{bA}(\vec{r}_{bA})\\&\times|\phi_a(\vec{r}_{bx})\chi_a^{(+)}(\vec{r}_{aA})\rangle+\langle\chi_b^{(-)}(\vec{r}_{bA})\chi_x^{(-)}(\vec{r}_{xA})|\\&\times U_{xA}(\vec{r}_{xA})+V_{xA}(\vec{r}_{xA})|\phi_a(\vec{r}_{bx})\chi_a^{(+)}(\vec{r}_{aA})\rangle\\&-\langle(\chi_b^{(-)}(\vec{r}_{bA})\chi_x^{(-)}(\vec{r}_{xA})|\phi_a(\vec{r}_{bx}))|U_{aA}(\vec{r}_{aA})\\&+V_{aA}(\vec{r}_{aA})|\chi_a^{(+)}(\vec{r}_{aA})\rangle\end{aligned} \tag{7}$$

$$=\mathscr{T}^b+\mathscr{T}^x-\mathscr{T}^a. \tag{8}$$

Here $\mathscr{T}^b$ and $\mathscr{T}^x$ represent the ''shearing'' due to the interaction of b and x with the target, respectively. The $\mathscr{T}^a$ term can be interpreted to provide the ''recombination'' as $(\chi_b^{(-)}\chi_x^{(-)}|\phi_a)$ gives the projectile component of the final state wave function, $\chi_b^{(-)}\chi_x^{(-)}$.

In the prior form DWBA prescription of Rybicki and Austern [11] the final state is taken as $\chi_{a*}^{(-)}\phi_{a*}$, where ϕ_{a*} is a continuum state of the projectile, and the recombination term becomes identically zero due to the orthogonality of ϕ_a and ϕ_{a*} [15].

From an inspection of Eq. (3) we find that for $d\rightarrow p+n$ breakup, the interaction potential in the form factor should be written as

$$U_{\text{int}}=(U_p+U_n-U_d)+(V_p-V_d), \tag{9}$$

whereas, in the prior form DWBA theory used by us

$$U_{\text{int}}=U_p+U_n+V_p \tag{10}$$

and the $\mathscr{T}$ matrix is

$$\mathscr{T}_{\text{DWBA}}^{\text{prior}}=\langle\chi_{d*}^{(-)}\phi_{d*}^{(-)}|U_p+U_n+V_p|\phi_d\chi_d^{(+)}\rangle. \tag{11}$$

Here, as explained earlier, the deuteron interaction part vanishes as the outgoing deuteron wave function ϕ_{d*} has no ground state component and the continuum states ϕ_{d*} are orthogonal to ϕ_d.

III. ANALYSIS

In this work we present the analysis of the 56 MeV $d \rightarrow p+n$ breakup data of Okamura *et al.* [1] with ^{12}C, ^{40}Ca, and ^{208}Pb targets. We used a modified version of the code of Goto [17, 18] which computes breakup cross section in the framework of the prior form DWBA theory of Rybicki and Austern [11]. In the ensuing calculations contributions from the maximum l values up to $l_{\max}=145$ and integration up to $R_{\max}=150$ fm are considered. In the following subsections analyses of the (d,pn) reaction with three different targets ^{12}C, ^{40}Ca and ^{208}Pb are presented separately. It is pertinent to note here that, even in our pure Coulomb breakup calculations, both nuclear and Coulomb distorted-waves have been utilized whereas, in the earlier calculation of Okamura *et al.* the distortion effects due to nuclear interaction between the target and the nucleons were neglected [1].

A. ^{12}C (d,pn)

The ^{12}C(d,pn) reaction data were taken at $\theta^L=\theta_p=\theta_n=0° - 55°$ and it was suggested by Okamura *et al.* [1] that the data above $\theta^L \sim 15°$ is strongly nuclear dominated. We studied the relative importance of the Coulomb and nuclear contributions at $\theta^L=0°,2°,4°,6°,10°,15°,25°$, and 35° and found that Coulomb part is usually smaller than the nuclear one except at $\theta^L=0°$ where the double-peaked Coulomb structure predominates (Fig. 1). Nevertheless, the Coulomb nuclear interference plays an important role at all forward angles including zero.

In our earlier work [18], we also found an overprediction at $\theta^L=15°$ and 0° when the usual optical potentials were used (Table I). Through a thorough parametric search it was found [18] that in order to get the best fit to both the shape and the magnitude of the energy sharing distribution data at $\theta^L=15°$, the real part of the exit channel nuclear potential had to be reduced from 65 MeV to 48 MeV.

The effect of variation of the energy integrated cross section $(d^2\sigma/d\Omega_p d\Omega_n)$ with the exit channel potential, V_{ex} (real part only), was systematically studied at $\theta^L=0°,6°,8°,10°,15°$, and 25° (Fig. 2). At $\theta^L=0°,6°,8°$, and 25° this variation has similar nature and the value of $d^2\sigma/d\Omega_p d\Omega_n$ at $V_{\text{ex}}=0$ MeV is less than that at $V_{\text{ex}}=65$ MeV. Interestingly, the nature of the above curve is totally opposite at $\theta^L=10°$ and 15° indicating a strong sensitivity of the present calculation to the exit channel potential near this region. The momentum transfer (i.e., the momentum difference between the incoming d and the scattered d^*) at $\theta^L=15°$ is around 117 MeV/c. In the 56 MeV ^{12}C(d,pn) reaction data a sudden drop in energy integrated cross section was found below this angle [1]. Incidentally, also in the $(^6\text{Li},\alpha d)$ breakup experimental data a similar dip in the cross section was found below this same momentum transfer value [19–23]. The similarity between these two entirely different systems is intriguing and might be a reflection of their basic S-wave structure of the bound state wave function as well as their similar and small binding energies. This aspects needs further exploration with other loosely bound nuclei.

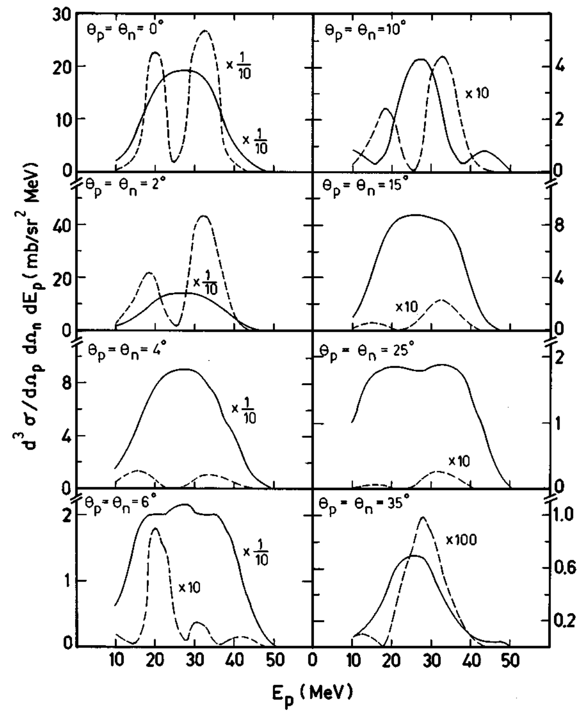

FIG. 1. Prior form DWBA calculations with the usual optical potentials (Table I) showing the relative contributions of the nuclear and Coulomb breakup in the energy sharing spectra of the 56 MeV ^{12}C(d,pn) reaction at different $\theta_p=\theta_n$. The solid lines represent calculations with only nuclear breakup and dashed lines represent with only Coulomb breakup calculations.

The variation of energy sharing spectra $(d^3\sigma/d\Omega_p d\Omega_n dE_p)$ with different exit channel potentials for $\theta^L=0°,6°,10°,15°,25°$ are shown in Fig. 3. At $\theta^L=15°$ the shape and magnitude of the energy sharing spectra are found to be quite sensitive to the exit channel potential whereas their effects are less drastic at $\theta^L=0°$.

We carried out the calculation of ^{12}C(d,pn) reaction at $\theta^L=15°$ with $V_{\text{ex}}=48$ MeV and 20 MeV separately, both of which yield approximately the same value of $d^2\sigma/d\Omega_p d\Omega_n$. The latter one produces an energy sharing distribution entirely different from the experimental data both in shape and in magnitude (Fig. 4). This observation proves that it is essential to have the energy sharing distribution data to accurately determine the exit channel potential and the energy integrated data alone is not sufficient for this purpose.

At $\theta^L=0°$ our pure Coulomb breakup calculation with full nuclear plus Coulomb distorted-waves at the entrance and the exit channels significantly overpredicts the data. Moreover it fails to reproduce the pronounced asymmetric structure of the energy sharing data (Fig. 5). This overprediction cannot be alleviated even if we reduce the exit channel potential to 0.0 MeV. Although the addition of the nuclear part in the form factor gives the correct asymmetric shape of the data, it largely overpredicts the overall magnitude of the energy sharing distribution (Fig. 6). This large

TABLE I. Optical potential parameters.

Reaction	E_{lab} (MeV)	V_0 (MeV)	r_0 (fm)	a_0 (fm)	W_v (MeV)	W_D (MeV)	r_I (fm)	a_I (fm)	r_c (fm)	Ref.
$d+{}^{12}$C	56	65.0	1.17	0.81	3.67	10.0	1.325	0.690	1.30	[12]
$p+{}^{12}$C	28	53.29	1.124	0.57	-	8.05	1.124	0.5	1.30	[12]
$n+{}^{12}$C	28	52.25	1.124	0.57	-	8.05	1.124	0.5	1.30	[12]
$d+{}^{40}$Ca	56	75.5	1.20	0.769	2.45	9.77	1.32	0.785	1.30	[25]
$p+{}^{40}$Ca	27.4	50.59	1.152	0.692	2.02	7.81	1.152	0.549	1.30	[26]
$n+{}^{40}$Ca	27.4	50.59	1.152	0.692	2.02	7.81	1.152	0.549	1.30	[26]
$d+{}^{208}$Pb	52	79.8	1.25	0.66	12.0	-	1.25	1.0	1.30	[27]
$p+{}^{208}$Pb	30	56.12	1.16	0.75	6.51	4.04	1.37	0.63	1.30	[28]
$n+{}^{208}$Pb	30	69.55	1.16	0.77	4.50	3.5	1.58	0.51	1.30	[28]

overprediction is sustained even if the exit channel potential is reduced to zero. In our earlier work [18] we did a search on the exit channel parameters $V_0(=V_{\mathrm{ex}}),r_0,a_0$ and found that the use of an unusually long range optical potential with reduced strength (V_0=55 MeV, r_0=4 fm, a_0=4 fm) gives a closer fit to the data. Nevertheless, there remains some scope for improvement.

A possible source of discrepancy might be the form factor used in the calculation where we used the on-shell $p+{}^{12}$C and $n+{}^{12}$C scattering potentials. The actual off-shell potentials could be different from the above values both in shape and in magnitude. In fact, in the 156 MeV ${}^6\mathrm{Li}\rightarrow\alpha+d$ breakup reaction studies with ^{208}Pb target, it was found that much shallower and spatially more extended transition potentials approximately reproduced the energy sharing data taken at wider angles [24]. In those calculations the Coulomb breakup part was neglected as it was expected to be small due to the large relative momenta between the fragments detected at wide angles. However, in the case of the $d\rightarrow p+n$ breakup reaction at $\theta^L=0°$ the Coulomb breakup is the most important ingredient and cannot be neglected. Interestingly, for the deuteron breakup the scattering cross section is found to be more sensitive to the variation of the strength of both the nuclear and the Coulomb transition potentials than the geometrical parameters and the large overpredictions can be adjusted by reducing only the depth of the transition potentials. Therefore, we multiplied the transition potentials by arbitrary reduction factors and adjusted their values to reproduce the data. We call the reduction factors of the nuclear and Coulomb transition potentials B_n and B_c, respectively. The possible implications of these reduction factors will be discussed in the next section.

At $\theta^L=15°$, the energy sharing data can be reasonably reproduced both by the usual optical potential (V_{ex}=65 MeV) with $B_n=B_c$=0.67 and by the unusual optical potential (V_{ex}=48 MeV) with $B_n=B_c$=1, the latter producing a

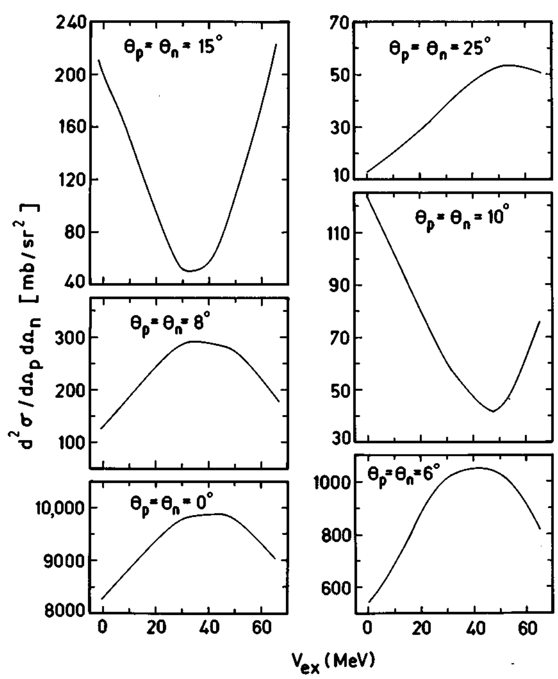

FIG. 2. Variation of energy integrated cross section with V_{ex} for the 56 MeV ${}^{12}\mathrm{C}(d,pn)$ reaction at different $\theta_p=\theta_n$.

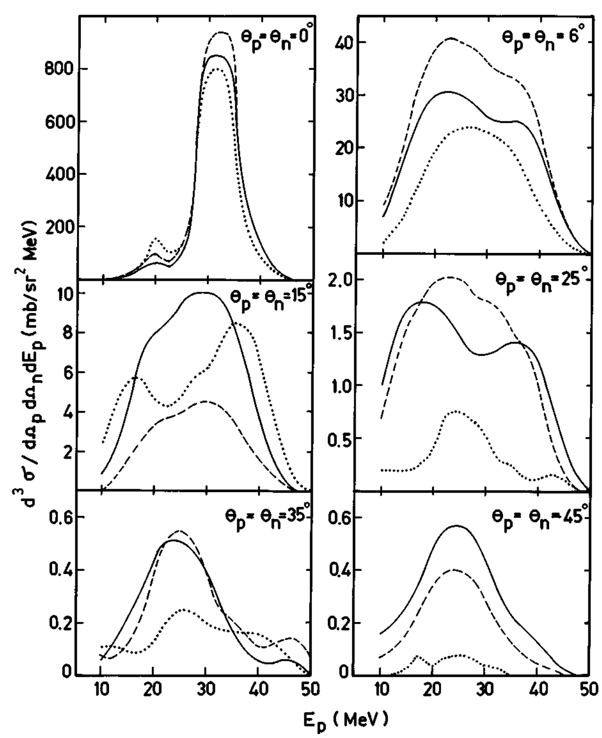

FIG. 3. Variation of energy sharing spectra with different exit channel potentials for the 56 MeV ${}^{12}\mathrm{C}(d,pn)$ reaction at different $\theta_p=\theta_n$. The solid, dashed, and dotted curves represent calculations with V_{ex} = 65 MeV, 48 MeV, and 0 MeV, respectively.

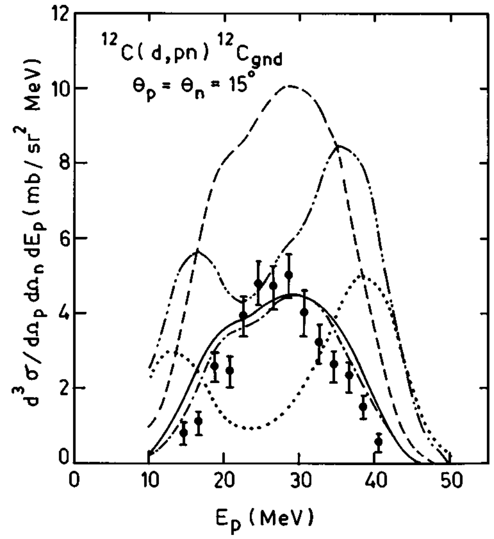

FIG. 4. Energy sharing spectra for the 56 MeV $^{12}C(d,pn)$ reaction at $\theta_p = \theta_n = 15°$. The dashed line shows the results of the usual optical potentials (unnormalized). The dash-double-dotted, dotted, and dash-dotted lines are with V_{ex}=0, 20, and 48 MeV (unusual optical potentials), respectively. The solid line represents calculations with usual optical potentials but $B_n = B_c = 0.67$.

slightly better fit to the experimental data (Fig. 4). Calculations with the reduction factors B_n=0.6, B_c=0.5, and V_{ex}=0.0 MeV, and $B_n = B_c = 1$ and V_{ex}=20 MeV also reproduce the energy integrated cross section but they fail to describe the energy sharing data and therefore discarded.

In contrast to the $\theta^L = 15°$ data, for $\theta^L = 0°$, no variation of V_{ex} with $B_n = B_c = 1$ reproduces the magnitude of either the energy sharing data or the energy integrated data. An excellent fit to the $\theta^L = 0°$ data is obtained using B_n=0.3 and

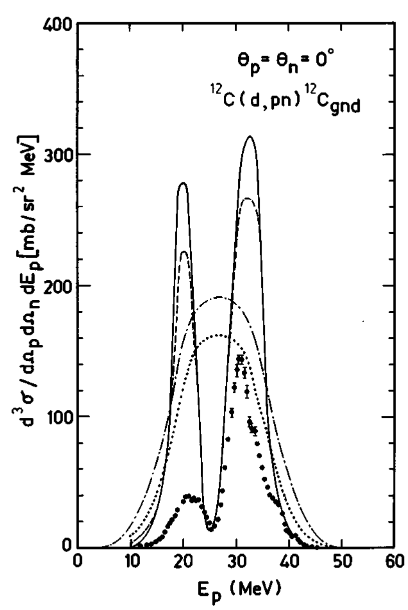

FIG. 5. Energy sharing spectra for $^{12}C(d,pn)$ reaction at $\theta_p = \theta_n = 0°$. The solid (dashed) line shows Coulomb breakup contribution for V_{ex}=0 MeV (V_{ex}=65 MeV). The dotted (dash-dotted) line shows the nuclear breakup contribution for V_{ex}=0 MeV (V_{ex}=65 MeV).

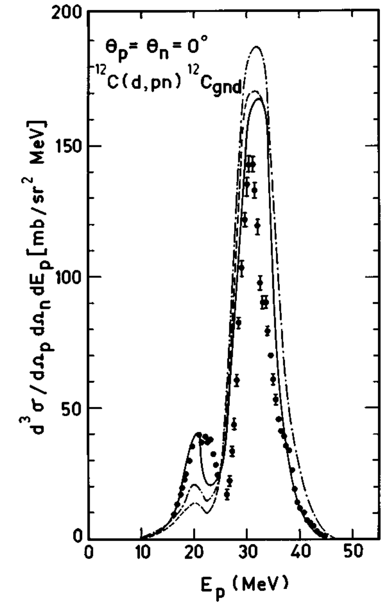

FIG. 6. Energy sharing spectra for the $^{12}C(d,pn)$ reaction at $\theta_p = \theta_n = 0°$ and full nuclear plus Coulomb breakup calculations with different exit channel potentials. The solid line is with V_{ex} =0 MeV, the dashed and dash-dotted lines are with V_{ex}=65 and 48 MeV, respectively. All results are shown after multiplying by a factor 0.2.

B_c=0.5 with V_d^{exit}=0.0 MeV only (Fig. 7).

At $\theta^L = 6°$, B_n=0.3 and B_c=0.3 with V_d^{exit}=0.0 MeV approximately reproduce the absolute magnitude of the available energy integrated data but, as explained above, the exact values of B_n and B_c, cannot be ascertained in the absence of the energy sharing data.

In summary, the $\theta^L = 15°$ data can be reproduced either by an unusual optical potential (V_{ex}=48 MeV) or by using

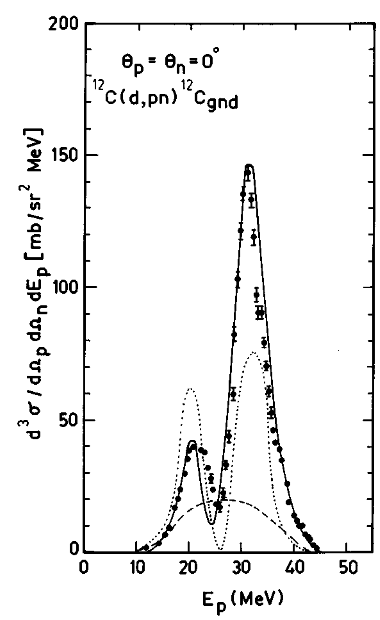

FIG. 7. Energy sharing spectra for the 56 MeV $^{12}C(d,pn)$ reaction at $\theta_p = \theta_n = 0°$. The solid line is with B_n=0.3, B_c=0.5, and V_{ex} =0 MeV. The dashed (dotted) line is for B_n=0.3, B_c=0, i.e., nuclear only (B_n=0, B_c=0.5, i.e., Coulomb only).

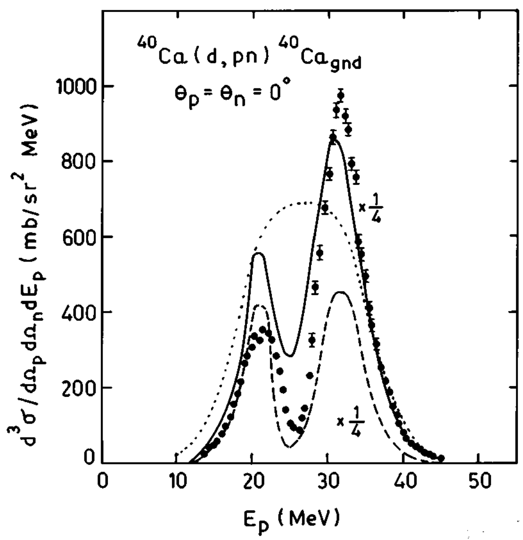

FIG. 8. Energy sharing spectra for the ^{40}Ca(d,pn) reaction at $\theta_p = \theta_n = 0°$ and calculations with usual optical potentials. The solid (dashed) line shows results with full nuclear plus Coulomb (Coulomb only) contributions shown multiplied by a factor of 1/4. The dotted line shows the result of nuclear breakup only.

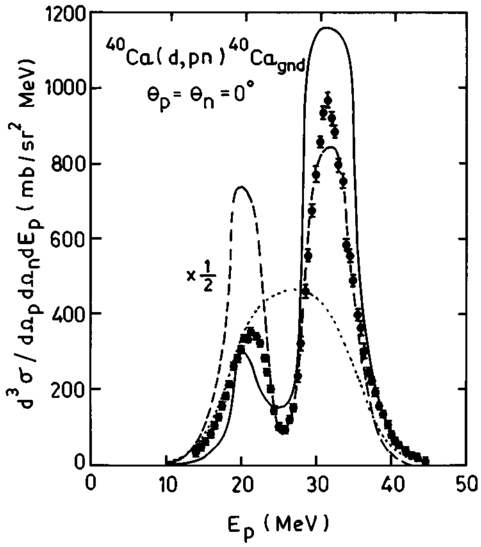

FIG. 9. Energy sharing spectra for the ^{40}Ca(d,pn) reaction at $\theta_p = \theta_n = 0°$. The solid line shows full nuclear plus Coulomb breakup results with unusual optical potentials. The dotted (dashed) line shows nuclear (Coulomb) contributions separately. The full nuclear plus Coulomb calculations are shown multiplied by a factor of 1/3 and the pure Coulomb part is shown multiplied by a factor of 1/2.

reduction factors $B_n = B_c = 0.67$ in the both nuclear and Coulomb transition potentials, the first choice being somewhat better. For $\theta^L = 0°$ the unusual potential as low as $V_{\rm ex} = 0$ MeV fails to reproduce the low cross section data and additional reduction factors ($B_n = 0.3$, $B_c = 0.5$) are needed to fit the data. The Coulomb nuclear interference effect is found to be significant at all the forward angles including zero.

B. ^{40}Ca(d,pn)

The (d,pn) data with ^{40}Ca target also show a double-peaked structure with pronounced asymmetry. Table I contains the optical potential parameters for the $d + {}^{40}$Ca scattering at 56 MeV and the $p + {}^{40}$Ca and $n + {}^{40}$Ca scattering at 28 MeV used in this analysis. With these parameters the pure Coulomb breakup calculations fail to reproduce both the shape and the magnitude of the triple differential cross section data. However, the pure Coulomb result dominates the pure nuclear one. Consideration of Coulomb plus nuclear breakup delineates some asymmetry but highly overpredicts the observed data. The Coulomb and nuclear plus Coulomb breakup calculations are shown in Fig. 8 both reduced by a factor of 4.

The magnitude and the shape of the triple differential cross section was found to be sensitive to the exit channel potential and after a systematic search a closer fit to the data could be obtained with $V_0 = 70$ MeV, $r_0 = 2$ fm, and $a_0 = 0.769$ fm. However, unlike the case of the ^{12}C target, here we had to use a further reduction factor of 3 to get a comparable magnitude (Fig. 9).

Alternatively, the correct magnitude could be reproduced by using the reduction factors $B_n = 0.4$, $B_c = 0.6$ in the form factors along with the unusual optical potential at the exit channel (Fig. 10).

It is pertinent to note that in the case of ^{12}C, at $\theta^L = 0°$, we got the best fit with $B_n = 0.3$, $B_c = 0.5$, and $V_{\rm ex} = 0.0$ MeV without changing the geometry parameters of the exit channel potential. This approach is found to be nonapplicable in the case of ^{40}Ca where in addition to $B_n = 0.4$, $B_c = 0.6$ and an unusually low $V_{\rm ex} = 70$ MeV, the geometry parameters of the exit channel potential also need to be altered in order to get the best fit to the data.

C. ^{208}Pb(d,pn)

The ^{208}Pb(d,pn) breakup data at $\theta^L = 0°$ show an extremly interesting feature where the expected double-peaked

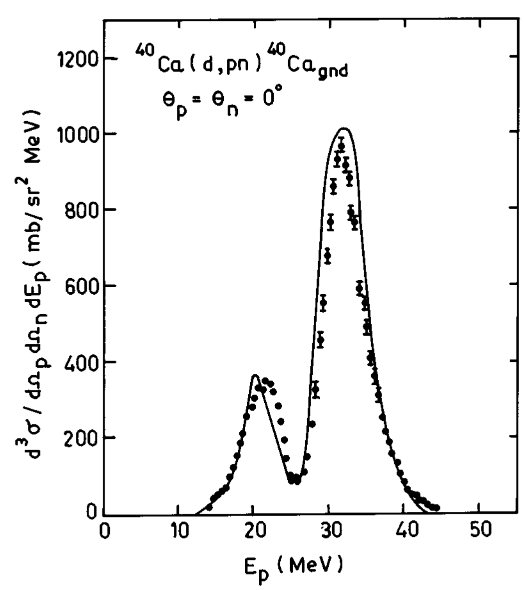

FIG. 10. Energy sharing spectra for the ^{40}Ca(d,pn) reaction at $\theta_p = \theta_n = 0°$. The solid line corresponds to nuclear plus Coulomb breakup calculations with $B_n = 0.4$, $B_c = 0.6$ and the same unusual optical potentials as in Fig. 9.

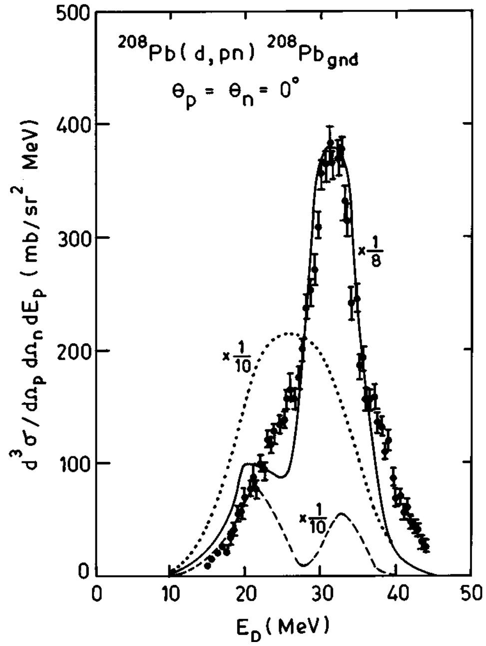

FIG. 11. Energy sharing spectra for ^{208}Pb(d,pn) reaction at $\theta_p = \theta_n = 0°$ and calculations with usual optical potentials. The solid line (dashed/dotted) shows results with full nuclear plus Coulomb (Coulomb only/nuclear only) contributions.

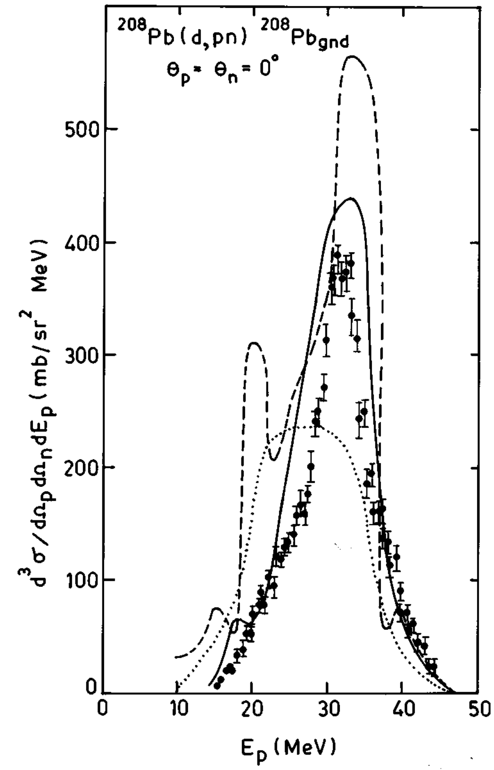

FIG. 12. Energy sharing spectra for the ^{208}Pb(d,pn) reaction at $\theta_p = \theta_n = 0°$. The solid line shows full nuclear plus Coulomb breakup result (normalized by a factor of 0.1) with an unusual optical potential. The dotted (dashed) line shows nuclear (Coulomb) contributions separately. The dominating nuclear part is shown reduced by a factor of 10.

structure of Coulomb dissociation vanishes and a prominent single peak is seen at higher proton energy.

From the pure Coulomb breakup calculation we find that instead of producing a single peak it generates the expected double-peaked structure (Fig. 11). This large deviation is somewhat puzzling as one expects the Coulomb breakup description to be more valid with the ^{208}Pb ($Z = 82$) target than the ^{12}C ($Z = 6$) target.

Interestingly, the nuclear breakup part here dominates the Coulomb breakup (Fig. 11) a feature not observed in the deuteron breakup at $\theta^L = 0°$ with ^{12}C and ^{40}Ca targets. Coulomb nuclear interference also does not reproduce the single-peaked structure and it highly overpredicts the overall magnitude of the energy sharing data (Fig. 11). The optical potential parameters are given in Table I.

The single-peaked structure can be reproduced by the use of unusual optical potential parameters ($V_0 = 70$ MeV, $r_0 = 1.5$ fm, $a_0 = 1.0$ fm) at the exit channel when both nuclear and Coulomb breakup are considered. This result is shown multiplied by a factor 0.1 in Fig. 12. Interestingly, the pure Coulomb calculations with the unusual optical potential fails to give the single-peaked structure. This indicates the importance of the Coulomb nuclear interference in ^{208} Pb. However, the exact magnitude of the data can be reproduced after an appropriate normalization factor is used in the Coulomb plus nuclear calculations. This renormalization can also be simulated by the reduction factors $B_n = 0.3$, $B_c = 0.3$ in the transition potentials (Fig. 13).

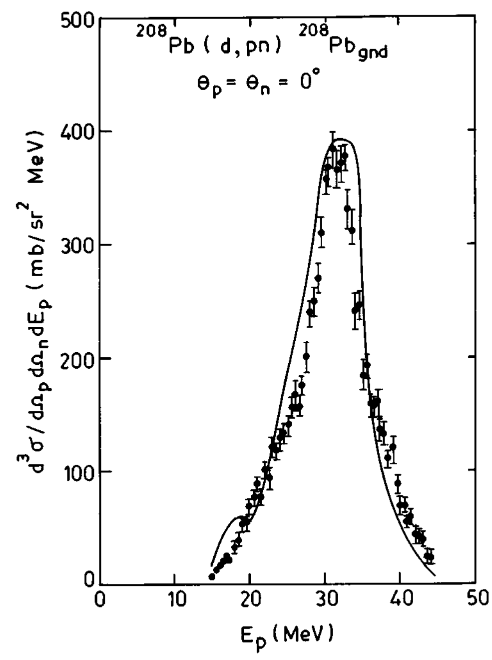

FIG. 13. Energy sharing spectra for the ^{208}Pb(d,pn) reaction at $\theta_p = \theta_n = 0°$. The solid line shows nuclear plus Coulomb breakup results with $B_n = B_c = 0.3$ and the same unusual optical potential as Fig. 12.

IV. CONCLUDING REMARKS

In this work a detailed analysis of the 56 MeV deuteron breakup data of Okamura *et al.* [1] with ^{12}C, ^{40}Ca, and ^{208}Pb targets in the framework of the prior form DWBA theory is presented with both usual and unusual optical potentials at the exit channel. The unusual optical potential is essentially the effective distorting potential for the broken-up deuteron in the exit channel which is related to the continuum-continuum coupling. The pure Coulomb breakup calculations both with usual and unusual optical potentials at the exit channel fail to describe the data. The addition of a nuclear breakup part in conjunction with the usual optical potentials at both entrance and exit channels also fail to reproduce the asymmetric structure of the $\theta_p = \theta_n = 0°$ data. An unusual optical potential at the exit channel along with reduction factors in the nuclear (real part only) and Coulomb transition potentials explain the data. For ^{40}Ca and ^{208}Pb the exit channel potentials are found to be highly deformed in shape while for ^{12}C only a reduced strength exit channel potential needs to be considered. For an accurate determination of the exit channel potential, the energy integrated cross section is found to be inadequate and the necessity of the energy sharing spectrum is established.

The reduction factors of the transition potentials might be simulating the off-shell effect of the fragment-target interaction for which we used the on-shell potentials. It was pointed out by Heide *et al.* [24] that the exact $\mathcal{T}$ matrix for the breakup in the prior form DWBA can be written as

$$\mathcal{T} = \langle \chi_{a*}^{(-)} \phi_k^{(-)} | (U_{bA} + U_{xA} - U_{aA}) \Omega | \chi_a^{(+)} \phi_a \rangle, \quad (12)$$

where U_{aA} is the exit channel distortion potential generating χ_a and Ω is similar to the Moeller's operator defined by

$$\Psi^{(+)} = \Omega \chi_a^{(+)} \phi_a . \quad (13)$$

If the breakup channel coupling effect is large, Ω will be different from unity. This of course is in addition to the inadequecy of the used breakup model itself, and to the fact that the scattering potential is in general nonlocal which is different from the local on-shell scattering potential. In this work, the fragments are on the same side of the beam at equal angles with small realtive breakup energies for which the coupling effects are expected to be large. The unusual optical potential at the exit channel may not be sufficient to simulate this large coupling effect at $\theta^L = 0°$. This inadequecy might be reflected in the additional requirement of the reduction factors B_n and B_c.

It is pertinent to note that in the prior form DWBA theory the outgoing deuteron wave function does not contain a ground state component which would be important if the recombination of $p + n \rightarrow d$ takes place. For deuteron breakup, Koike discussed the effect of the FSI in the quasi-free scattering (QFS) region to explain the supression of the QFS peaks at forward angles in the three-body model [29]. He gave the theoretical explanation of the effect of the FSI in the QFS region on the $\alpha + d \rightarrow \alpha + n + p$ reaction spectra and his idea is partly confirmed by the ^{2}H$(\alpha, \alpha p)n$ data [30] at $E_\alpha = 140$ MeV. In the $d + d \rightarrow d + n + p$ system, a similar supression of the QFS peak was reported by Klug *et al.* [31]. The deuteron wave function has a large span in radial space owing to its small binding energy. Therefore, the recombination might occur due to strong attractive force between the fragments when their relative energy (ϵ) is small. At large impact parameter, the recombination effect due to attractive nuclear force between the fragments might dominate over the disruptive but weak breakup force. Therefore, at $\theta^L = 0°$ the FSI between the fragments (going in the same direction with low relative energies) may induce ''recombination'' which could contribute in the reduction of the breakup cross section. The present analysis with the single-step DWBA formalism can only point out these possibilities, but it cannot prove such a FSI conclusively as the recombination effect is not incorporated in the present formalism.

We would like to stress here that we do not claim that our calculated cross sections with the normalization factors B_n and B_c provide the exact theoretical interpretation of the reaction mechanism. But, the requirement of the normalization factors, B_n and B_c, strongly points at the existence of a large reduction of breakup cross sections at the extreme forward angle, indicating the presence of an additional reaction mechanism. This reduction cannot be reproduced by the single-step DWBA theory even with unusual optical potentials in the exit channel, although, this last prescription [15] does explain the data at angles beyond a certain critical momentum transfer ($\sim$117 MeV/c). This aspect possibly needs to be considered in all the Coulomb dissociation calculations as it might affect the extraction of the astrophysical S factors. For a proper understanding of the actual reaction mechanisms, a full three-body theory with multistep processes is needed.

In conclusion, we find that at $\theta^L = 0°$, as suggested by Okamura *et al.*, [1] the Coulomb dissociation indeed dominates the $d \rightarrow p + n$ breakup reaction in the case of ^{12}C and ^{40}Ca targets while, for the heavier ^{208}Pb target, the nuclear breakup is the dominant one. Nevertheless, the Coulomb nuclear interference cannot be ignored even in ^{12}C or ^{40}Ca target. In the context of Coulomb dissociation measurements, the failure of the one-step pure Coulomb breakup formalism at 56 MeV incident deuteron energy is an important finding which suggests that the Coulomb dissociation of deuterons should be explored in other energy domains for its fruitful utilizations in astrophysics.

ACKNOWLEDGMENT

We are thankful to H. Okamura for sending us his 56 MeV deuteron breakup data of [1] in a tabular form.

[1] H. Okamura, H. Hatori, N. Matsuoka, T. Noro, A. Okihana, H. Sakai, H.M. Shimizu, K. Takeshita, and T. Yamaya, Phys. Lett. B **325**, 308 (1994).

[2] G. Baur, C.A. Bertulani, and H. Rebel, Nucl. Phys. **A459**, 188 (1986).

[3] G. Baur and H. Rebel, J. Phys. G **20**, 1 (1994).

[4] L.F. Canto, R. Donangelo, A. Romanelli, and H. Schulz, Phys. Lett. B **318**, 415 (1993).

[5] F. Barranco, E. Vigezzi, and R.A. Broglia, Phys. Lett. B **319**, 387 (1983).

[6] F.L.H. Wolfs, C.A. White, D.C. Bryan, C.G. Freeman, D.M. Herrick, K.L. Kurz, D.H. Mathews, P.A.A. Perera, and M.T. Zanni, Phys. Rev. C **49**, 2538 (1994).
[7] L.S. Ferreira, E. Maglione, J.M. Bang, I.J. Thompson, B.V. Danilin, M.V. Zhukov, and J.S. Vaagen, Phys. Lett. B **316**, 23 (1993).
[8] H. Rebel, in *Frontier Topics in Nuclear Physics*, edited by W. Scheid and A. Sandulescu (Plenum Press, New York, 1994).
[9] I. Tanihata, Nucl. Phys. **A553**, 361c (1993).
[10] G. Baur, F. Rosel, and D. Trautmann, Nucl. Phys. **A265**, 101 (1976); G. Baur and D. Trautmann, Phys. Rep. C **25**, 293 (1976); G. Baur, F. Rosel, D. Trautmann, and R. Shyam, *ibid.* **111**, 333 (1984).
[11] Frank Rybicki and N. Austern, Phys. Rev. C **6**, 1525 (1972).
[12] N. Matsuoka, K. Hatanaka, T. Saito, T. Itahasi, K. Hosono, A. Shimizu, M. Kondo, F. Ohotani, and O. Cynshi, Nucl. Phys. **A391**, 357 (1982).
[13] Y. Iseri, M. Yahiro, and M. Kamimura, Prog. Theor. Phys. Suppl. **89**, 84 (1986).
[14] N. Austern, Y. Iseri, M. Kamimura, M. Kawai, G. Rawitscher, and M. Yahiro, Phys. Rep. **154**, 125 (1987).
[15] N. Austern, Phys. Rev. C **30**, 1130 (1984).
[16] D.K. Srivastava and H. Rebel, Phys. Rev. C **33**, 1221 (1986); D.K. Srivastava, KfK Report 4007, 1985.
[17] A. Goto, H. Kamitsubo, N. Matsuoka, and H. Sakaguchi, Nucl. Phys. **A444**, 248 (1985).
[18] C. Samanta, Rituparna Kanungo, Sanjukta Mukherjee, and D.N. Basu, Phys. Lett. B **352**, 197 (1995).
[19] C. Samanta, Sudip Ghosh, M. Lahiri, S. Ray, and S.R. Banerjee, Phys. Rev. C **45**, 1757 (1992).
[20] C. Samanta, M. Lahiri, Subinit Roy, S. Ray, and S.R. Banerjee, Phys. Rev. C **47**, 1313 (1993).
[21] C. Samanta, T. Sinha, Sudip Ghosh, S. Ray, and S.R. Banerjee, Phys. Rev. C **50**, 1226 (1994).
[22] M. Tosaki, M. Fujiwara, K. Hosono, T. Noro, H. Ito, T. Yamazaki, and H. Ikegami, Nucl. Phys. **A493**, 1 (1989).
[23] J. Kiener, G. Gsottschneider, H.J. Gils, H. Rebel, V. Corcalciuc, S.K. Basu, G. Baur, and J. Raynal, Z. Phys. A **339**, 489 (1991).
[24] N. Heide, D.K. Srivastava, and H. Rebel, Phys. Rev. Lett. **63**, 601 (1989); D.K. Srivastava, H. Rebel, and N. Heide, Nucl. Phys. **A506**, 346 (1990).
[25] N. Matsuoka, H. Sakai, T. Saito, K. Hosono, M. Kondo, H. Ito, K. Hatanaka, T. Ichihara, A. Okihana, K. Imai, and K. Nisimura, Nucl. Phys. **A455**, 413 (1986).
[26] W.T.H. van Oers, Phys. Rev. C **3**, 1550 (1971).
[27] F. Hinterberger, G. Mairle, U. Schmidt-Rohr, G.J. Wagner, and P. Turek, Nucl. Phys. **111**, 265 (1968).
[28] M.P. Fricke, E.E. Gross, B.J. Morton, and A. Zuker, Phys. Rev. **156**, 1207 (1967); **147**, 812 (1966).
[29] Y. Koike, Ph.D thesis, Kyoto University, 1978 (unpublished); M. Tosaki, Ph.D thesis, Osaka University, 1989 (unpublished).
[30] J.M. Lambert, P.A. Treado, P.G. Roos, N.S. Chant, A. Nadasen, I. Slaus, and Y. Koike, Phys. Rev. C **26**, 357 (1982).
[31] W. Klug, H. Matthay, R. Schlufter, and K. Wick, Nucl. Phys. **A302**, 93 (1978).